Chinese Chemical Letters 33 (2022) 2550–2554

Contents lists available at ScienceDirect

Chinese Chemical Letters

journal homepage: www.elsevier.com/locate/cclet

Development of peptidomimetic hydroxamates as *Pf*A-M1 and *Pf*A-M17 dual inhibitors: Biological evaluation and structural characterization by cocrystallization

Anil Kumar Marapaka[a,b,c,1], Priyanka Sankoju[b,c,1], Guozhen Zhang[a,1], Yongzheng Ding[a,1], Chunhua Ma[a], Vijaykumar Pillalamarri[b,c], Renu Sudhakar[d], Bharati Reddi[b,c], Puran Singh Sijwali[d,*], Yingjie Zhang[a,*], Anthony Addlagatta[b,c,*]

[a] *Department of Medicinal Chemistry, Key Laboratory of Chemical Biology (Ministry of Education), School of Pharmaceutical Sciences, Cheeloo College of Medicine, Shandong University, Ji'nan 250012, China*
[b] *Department Applied Biology, CSIR-Indian Institute of Chemical Technology, Tarnaka, Hyderabad, Telangana-500 007, India*
[c] *Academy of Scientific and Innovative Research (AcSIR), Ghaziabad-201002, India*
[d] *CSIR-Centre for Cellular and Molecular Biology, Tarnaka, Hyderabad, Telangana-500 007, India*

ARTICLE INFO

Article history:
Received 28 July 2021
Revised 15 September 2021
Accepted 29 September 2021
Available online 4 October 2021

Keywords:
Aminopeptidase
Dual inhibitor
Antimalaria
Peptidomimetic
Plasmodium falciparum

ABSTRACT

Plasmodium parasites causing malaria have developed resistance to most of the antimalarials in use, including the artemisinin-based combinations, which are the last line of defense against malaria. This necessitates the discovery of new targets and the development of novel antimalarials. *Plasmodium falciparum* alanyl aminopeptidase (*Pf*A-M1) and leucyl aminopeptidase (*Pf*A-M17) belong to the M1 and M17 family of metalloproteases respectively and play critical roles in the asexual erythrocytic stage of development. These enzymes have been suggested as potential antimalarial drug targets. Herein we describe the development of peptidomimetic hydroxamates as *Pf*A-M1 and *Pf*A-M17 dual inhibitors. Most of the compounds described in this study display inhibition at sub-micromolar range against the recombinant *Pf*A-M1 and *Pf*A-M17. More importantly, compound **26** not only exhibits potent malarial aminopeptidases inhibitory activities (*Pf*A-M1 K_i = 0.11 ± 0.0002 μmol/L, *Pf*A-M17 K_i = 0.05 ± 0.005 μmol/L), but also possesses remarkable selectivity over the mammalian counterpart (*p*APN K_i = 17.24 ± 0.08 μmol/L), which endows **26** with strong inhibition of the malarial parasite growth and negligible cytotoxicity on human cell lines. Crystal structures of *Pf*A-M1 at atomic resolution in complex with four different compounds including compound **26** establish the structural basis for their inhibitory activities. Notably, the terminal ureidobenzyl group of **26** explores the S2′ region where differences between the malarial and mammalian enzymes are apparent, which rationalizes the selectivity of **26**. Together, our data provide important insights for the rational and structure-based design of selective and dual inhibitors of malarial aminopeptidases that will likely lead to novel chemotherapeutics for the treatment of malaria.

Malaria, the world's most prevalent parasitic disease, is caused by the protozoan parasite called *Plasmodium* [1]. According to the World Malaria Report 2020, the number of malaria cases exceeded 220 million and around 400,000 deaths from malaria occurred in 2019, mostly children in Africa [2]. Traditional chemotherapeutic strategies for malaria control can be categorized mainly into three types: quinoline-related compounds (quinine, quinidine, chloroquine, mefloquine, *etc.*), antifolate compounds (proguanil, pyrimethamine, trimethoprim, *etc.*) and artemisinin derivatives (artemisinin, dihydroartemisinin, artesunate, artemether, arteether, *etc.*) [3]. Unfortunately, the emergence and widespread of resistant *Plasmodium falciparum* to most of the currently available antimalarials is alarming and necessitates development of novel antimalarial drugs [1,3].

Hemoglobin digestion is an essential metabolic process in the intraerythrocytic stage of the *Plasmodium* life cycle. During this process, malaria parasites digest host cell hemoglobin to get amino acids required for parasite protein synthesis [4,5]. Among kinds of metalloami-nopeptidases involved in hemoglobin digestion in

* Corresponding authors.
E-mail addresses: zhangyingjie@sdu.edu.cn (Y. Zhang), anthony@csiriict.in (A. Addlagatta), psijwali@ccmb.res.in (P.S. Sijwali).
[1] These authors contributed equally to this work.

https://doi.org/10.1016/j.cclet.2021.09.102
1001-8417/

Plasmodium falciparum, alanyl aminopeptidase (*Pf*A-M1) and leucyl aminopeptidase (*Pf*A-M17) are two important contributors of single amino acid generation from shorter peptides generated by endopeptidases [6]. *Pf*A-M1 has been demonstrated to cleave hydrophobic and positively charged amino acids with best preference to leucine, alanine, arginine and phenylalanine [7]. On the other hand, *Pf*A-M17 has much narrower substrate specificity exhibiting a strong preference for N-terminal hydrophobic residues, in particular leucine and tryptophan [7]. It is worth noting that gene knockout and specific inhibition of *Pf*A-M1 and *Pf*A-M17 from *Plasmodium falciparum* were lethal, indicating they are ideal drug targets [8,9]. Given that both *Pf*A-M1 and *Pf*A-M17 are potential drug targets, several attempts were made to target these two metalloaminopeptidases individually or together by various types of small molecules, which could be mainly categorized into hydroxamates [10–15], phosphates/phosphinates [16–19], amino–benzosuberones [20,21] and bestatin analogs [9,22]. Generally, inhibitors that consist of hydroxamate moiety as the zinc-binding group (ZBG) exhibited potent aminopeptidases inhibitory activities and were capable of reaching the site of action within infected red blood cells to exert antimalarial effects [10–15]. For example, compounds **1, 2** and **3** were reported to be potent *Pf*A-M1 inhibitors, among which **1** and **2** exhibited moderate *in vitro* antimalarial activities [10, 11]. Compounds **4** and **5** could inhibit *Pf*A-M1 and *Pf*A-M17 simultaneously and showed promising *in vitro* antimalarial activities [12,13]. Moreover, another *Pf*A-M1 and *Pf*A-M17 dual inhibitor **6** showed oral efficacy against murine malaria [14] (Fig. S1 in Supporting information).

In our previous work, we developed a series of leucine-derived hydroxamates (Fig. S2 in Supporting information) with potent inhibitory activities against mammalian aminopeptidase N (APN) [23,24]. Considering the structural similarity between the leucine-derived hydroxamates and the reported *Pf*A-M1 inhibitor **3** (Fig. S2), we speculated that these leucine-derived hydroxamates could also inhibit *Pf*A-M1 and even *Pf*A-M17, hence used as antimalarial lead compounds. In the present work, twelve leucine-derived hydroxamates were progressed to *in vitro* malarial aminopeptidases inhibition assay, which confirmed their potent *Pf*A-M1 and *Pf*A-M17 inhibitory activities. Structural characterization by cocrystallization of three compounds (**8**, **11** and **18**) revealed their binding modes in *Pf*A-M1. Compounds **8** and **18** adopted similar binding modes in the active site of *Pf*A-M1, with their benzyl and isobutyl groups occupying the S1 and S1′ pockets, respectively. Surprisingly, compound **11** bound in *Pf*A-M1 with its isobutyl group in the S1 pocket, its benzyl group reaching into the substrate/product access channel (indicated as the S2′ region), while leaving the S1′ pocket unoccupied. Based on the different binding modes, we suggested that compounds capable of interacting with S1, S1′ pockets and S2′ region simultaneously should exhibit improved malarial aminopeptidases inhibitory activity and selectivity. Therefore, a series of novel peptidomimetic hydroxamates were designed, synthesized and biologically evaluated. Satisfyingly, compound **26** stood out as a potent *Pf*A-M1 and *Pf*A-M17 dual inhibitor with *in vitro* antimalarial activities. Notably, compound **26** showed significant selectivity over the mammalian counterpart porcine aminopeptidase N (*p*APN), which could be rationalized by cocrystal structure analysis.

The leucine-derived hydroxamates **7**–**18** were previously reported as potent mammalian APN inhibitors with half inhibition concentration (IC_{50}) values against *p*APN in the low micromolar to nanomolar range [23,24]. In this study, the malarial aminopeptidases inhibitory activities of compounds **7**–**18** were evaluated against both *Pf*A-M1 and *Pf*A-M17 with bestatin as the positive control. The results listed in Table 1 showed that all leucine-derived hydroxamates possessed moderate to potent inhibitory activities against both malarial aminopeptidases. Overall, most compounds showed preference against *Pf*A-M1 over *Pf*A-M17. For example, compounds **7**, **11**, **13**, **15** and **16** inhibited *Pf*A-M1 with over 10-fold greater affinity than *Pf*A-M17. Since the main purpose of current research was identification of *Pf*A-M1 and *Pf*A-M17 dual inhibitors as antimalarial agents, we focused our attention on compounds **8**, **17** and **18**, which displayed potent and balanced *Pf*A-M1 and *Pf*A-M17 dual inhibition. It is worth noting that the malarial aminopeptidases inhibitory activities of compounds **8**, **17** and **18** were more potent than bestatin, therefore, they were progressed to cocrystallization study to provide the basis for rational design of more potent malarial aminopeptidases inhibitors.

Table 1
*Pf*A-M1 and *Pf*A-M17 inhibitory activities of compounds **7**–**18**.

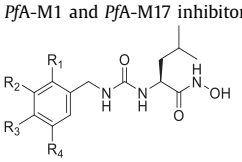

Compound	R_1	R_2	R_3	R_4	K_i (μmol/L) [a]	
					*Pf*A-M1	*Pf*A-M17
7	F	H	H	H	0.66 ± 0.0006	6.55 ± 0.04
8	Cl	H	H	H	0.41 ± 0.0001	0.78 ± 0.006
9	Br	H	H	H	0.59 ± 0.001	1.37 ± 0.03
10	CH_3	H	H	H	0.22 ± 0.004	1.18 ± 0.05
11	H	Cl	H	H	0.23 ± 0.001	2.42 ± 0.001
12	H	CH_3	H	H	0.37 ± 0.0005	2.72 ± 0.01
13	F	H	H	F	1.13 ± 0.001	15.05 ± 0.32
14	Cl	H	H	Cl	0.93 ± 0.0002	7.55 ± 0.29
15	F	H	F	H	0.35 ± 0.003	7.83 ± 0.30
16	OCH_3	H	OCH_3	H	0.61 ± 0.04	9.09 ± 0.003
17	H	CH_3	CH_3	H	0.12 ± 0.0001	0.10 ± 0.02
18	CH_3	CH_3	H	H	0.57 ± 0.0002	0.34 ± 0.20
Bestatin	/	/	/	/	0.90 ± 0.0005	1.39 ± 0.04

[a] Assays were performed in replicates ($n \geq 3$), values are shown as mean ± standard deviation (SD).

We have successfully determined the crystal structures of *Pf*A-M1 in complex with compounds **8** and **18** at atomic resolution (Figs. 1A and B and Table S1 in Supporting information). Our attempts to crystallize the *Pf*A-M17 in complex with inhibitors did not yield diffraction quality crystals. As shown in Figs. 1A and B, compounds **8** and **18** adopt similar binding modes in the active site of *Pf*A-M1, where the hydroxamate group bidentately coordinates the catalytic Zn^{2+}, and the benzyl and isobutyl groups interact with S1 and S1′ pockets, respectively. Moreover, both compounds **8** and **18** can form two hydrogen bonds with Y580 *via* the carbonyl O of hydroxamate group and the ureido NH that is close to the isobutyl group. Note that the binding poses of benzyl groups of compounds **8** and **18** in the S1 pocket are different. To be specific, the chlorobenzyl group of **8** is sandwiched between Y575 and M1034, forming π-π stacking interaction with Y575, hydrogen bond with A320, and hydrophobic interactions with V459, M1034, E572 and E319 (Fig. 1A). In contrast, the dimethylbenzyl group of **18** rotates dramatically and forms π-π T-shaped interaction with Y575, probably to avoid steric clashes resulting from the dimethyl substituents (Fig. 1B). The rotation of dimethylbenzyl group leads to a flip of the side chain of M1034, which might account for the slightly decreased potency of **18** compared with **8**. The isobutyl group of both compounds **8** and **18** reaches into the S1′ pocket outlined by V459, G460, V493, H496 and Y580. Although not fully occupying the S1′ pocket, the isobutyl group can form hydrophobic interactions with V459, G460 and Y580 (Figs. 1A and B).

The cocrystal structure of compound **11**, a *meta*–chloro-substituted isomer of **8** was also resolved (Fig. 1C and Table S1). Surprisingly, the binding mode of compound **11** in *Pf*A-M1 is quite different from that of compound **8**. Comparing Figs. 1A and C, it

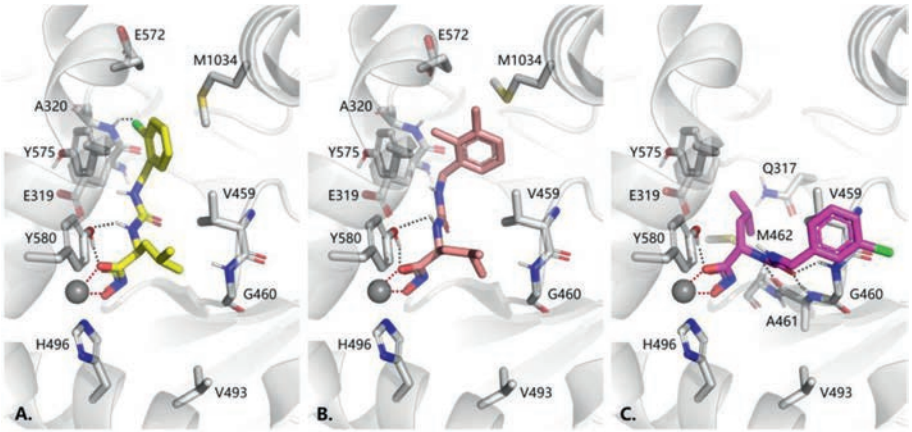

Fig. 1. The binding modes of compounds **8** (yellow, Fig. 1A, PDB: 5Y1K), **18** (pink, Fig. 1B, PDB: 5Y1T) and **11** (purple, Fig. 1C, PDB: 5Y1Q) in the active site of *Pf*A-M1 (gray cartoon and sticks). The zinc ion coordination and hydrogen bonds are indicated by red and black dashed lines, respectively.

is found that the isobutyl and benzyl groups of **11** rotate about 180° around the C–Cα bond relative to compound **8**. As a result, the isobutyl group of **11** moves out of S1′ pocket into the S1 pocket, wherein it points to the backwall of S1 pocket (M462, E319 and Q317) and forms hydrophobic interactions with V459 and Y575. However, the chlorobenzyl group of **11** could not occupy the S1′ pocket due to its steric bulk. Instead, the chlorobenzyl group reaches beyond the S1′ pocket and into the substrate/product access channel (S2′ region). It is worth noting that the ureido moiety of compound **11** forms three hydrogen bonds with G460 and A461, which are not observed in compounds **8** and **18**. However, the *Pf*A-M1 inhibitory activity of **11** (K_i = 0.23 ± 0.001 μmol/L) is only marginally increased relative to **8** (K_i = 0.41 ± 0.0001 μmol/L) and **18** (K_i = 0.57 ± 0.0002 μmol/L), which could be ascribed to its lack of interaction with the S1′ pocket.

Although the malarial aminopeptidases inhibitory potency of our previous leucine-derived hydroxamates have been confirmed, there are two problem s of these compounds. First, they show limited selectivity over mammalian aminopeptidase. Secondly, their malarial aminopeptidases inhibitory potency, especially against *Pf*A-M17, needs to be further improved. Structural characterization by cocrystallization revealed that these compounds use hydroxamate group to chelate the catalytic Zn^{2+}, which is crucial to their potency. It is worth noting that all these compounds can only occupy two of the three pockets/regions (S1, S1′ and S2′) in *Pf*A-M1 due to their simple structures (Table 2). We wondered if compounds capable of occupying S1, S1′ pockets and S2′ region simultaneously could exhibit improved malarial aminopeptidases inhibitory activity and selectivity. Therefore, a novel series of peptidomimetic hydroxamates were designed, hoping their three branched side chains could occupy the S1, S1′ pockets and the S2′ region simultaneously (Table 2).

Compounds **19**–**24** were prepared following the procedures described in Scheme S1 (Supporting information). The amino acid methyl ester hydrochlorides **A1**–**3** were condensed with pyrazinecarboxylic acid to give **B1**–**3**, which were hydrolyzed to give **C1**–**3**, respectively. Condensation of Boc-protected amino acid **E1**–**3** with L-leucine methyl ester hydrochloride gave intermediate **F1**–**3**, which upon deprotection afforded **G1**–**3**, respectively. Condensation of **C1**–**3** with L-leucine methyl ester hydrochloride, and condensation of **G1**–**3** with pyrazinecarboxylic acid, gave the common intermediates **D1**–**6**, which were reacted with NH_2OK in methanol to give target compounds **19**–**24**, respectively.

Compounds **25** and **26** were prepared following the procedures described in Scheme S2 (Supporting information). Condensation of **C2** and L-phenylalanine methyl ester hydrochloride led to **D7**, which was converted into compound **25** with NH_2OK in methanol. Intermediate **G4** was obtained from Boc-L-leucine and D-phenylglycine methyl ester hydrochloride using the similar method of synthesizing **G1**–**3**. Then **G4** was connected with benzylamine in the presence of triphosgene to give **H**, which was further reacted with NH_2OK in methanol to give target compound **26**.

The newly synthesized compounds **19**–**26** were progressed to malarial aminopeptidases inhibition assay with bestatin as the positive control. Unsatisfactorily, compounds **19**–**25** showed dramatically decreased inhibitory activities against both malarial and mammalian enzymes compared to **7**–**18** (Table 2). Among analogs **19**–**25**, only compound **22** with R_1 being H exhibited moderate *Pf*A-M17 inhibitory activity (K_i = 6.96 μmol/L). We speculated that these compounds could not fit well in the enzyme active sites due to steric hindrance resulting from their unsuitable geometry. In contrast, compound **26** with ureido-attached benzyl group, showed remarkable malarial aminopeptidases dual inhibition (*Pf*A-M1 K_i = 0.11 μmol/L, *Pf*A-M17 K_i = 0.05 μmol/L), which were more potent than bestatin and all parent leucine-derived hydroxamates (Table 1). It is worth noting that compound **26** displayed significantly improved *Pf*A-M17 activity compared to most leucine-derived hydroxamates. More importantly, compound **26** showed about 340-fold selectivity towards *Pf*A-M17, 150-fold selectivity towards *Pf*A-M1 over their mammalian counterpart *p*APN. The positive control bestatin is a pan-aminopeptidases inhibitor with some preference to *p*APN.

The crystal structure of *Pf*A-M1–**26** complex was determined at 1.96 Å (Fig. 2 and Table S1). As expected, compound **26** also coordinates the catalytic Zn^{2+} through the hydroxamate group. The hydrogen bond with Y580 is reserved. More importantly, it can interact with S1, S1′ pockets and S2′ region simultaneously (Fig. 2). To be specific, the phenyl group adjacent to the hydroxamate group is sandwiched between Y575 and V459 in S1 pocket, forming π-π stacking interaction with Y575 and π-σ interaction with V459. The amide O forms dual hydrogen bonds with G460 and A461, which facilitates the hydrophobic isobutyl group to occupy the S1′ pocket, wherein it interacts with the π electrons of H496 and forms hydrophobic interactions with V493 and T492. Remarkably, the ureido-attached benzyl moiety of **26** effectively explores the S2′ region, forming amide-π stacking interaction with the amide moiety connecting T576 and T577.

Since we did not get the cocrystallization of the *Pf*A-M17 and compound **26**, molecular docking was used to investigate the binding mode of compound **26** in *Pf*A-M17. As shown in Fig. S3A (Supporting information), compound **26** could fit well in the active site of *Pf*A-M17, with the hydroxamate group chelating the catalytic

Table 2
Design strategy of novel peptidomimetic hydroxamates **19**–**26** and their inhibition data against *Pf*A-M1, *Pf*A-M17 and *p*APN.

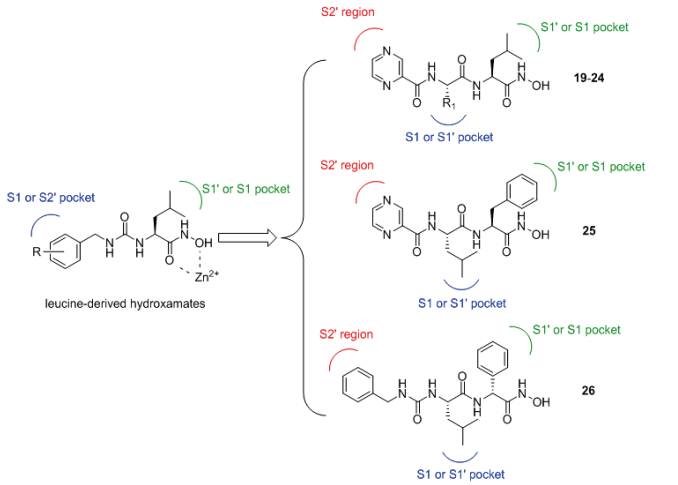

Compound	R_1	K_i (μmol/L)[a]		
		*Pf*A-M1	*Pf*A-M17	*p*APN
19		20.85 ± 0.02	106.97 ± 0.08	173.3 ± 0.2
20		37.55 ± 0.11	102.2 ± 0.26	87.51 ± 0.53
21		22.68 ± 0.72	119.37 ± 0.45	85.33 ± 0.22
22	H	18.19 ± 0.72	6.96 ± 0.20	42.42 ± 1.53
23	CH_3	42.63 ± 0.32	300.4 ± 0.1	49.4 ± 0.1
24	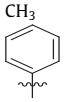	50.09 ± 1.32	121.47 ± 0.3	82.16 ± 1.09
25	/	93.31 ± 3.96	153.1 ± 0.5	145.9 ± 1.06
26	/	0.11 ± 0.0002	0.05 ± 0.005	17.24 ± 0.08
Bestatin	/	0.90 ± 0.0005	1.39 ± 0.04	0.05 ± 0.001

[a] Assays were performed in replicate (n ≥ 3), values are shown as mean ± SD.

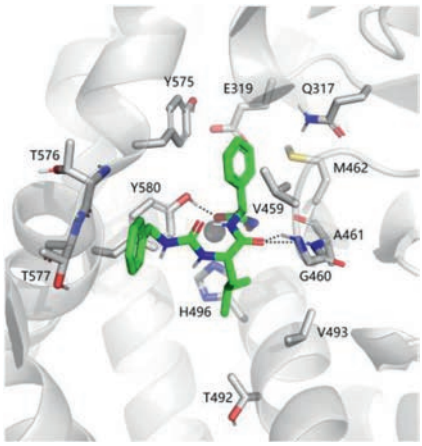

Fig. 2. The binding mode of compound **26** (green, PDB: 5XM7) in the active site of *Pf*A-M1 (gray cartoon and sticks). The hydrogen bonds are indicated by black dashed lines. The zinc ion coordination is omitted for clarity.

and regulatory zinc ions simultaneously. The coordination between the hydroxamate group and the two zinc ions are clearly presented in Fig. S3B (Supporting information). Similar to its binding mode in *Pf*A-M1, compound **26** could interact with the S1, S1′ pockets and the S2′ region of *Pf*A-M17 *via* its phenyl, isobutyl and benzyl groups, respectively. To be specific, the phenyl group of **26** is sandwiched between M396 and G489 in the S1 pocket, forming hydrophobic interactions with F398, L492 and A577. The isobutyl group partially occupies the S1′ pocket bordered by A460, N457, I547 and S554. The ureido-attached benzyl group is projected to the solvent-exposed S2′ region, interacting with the loop consist of N384, L385, K386, A387 and A388 (Fig. S3A). Remarkably, compound **26** could form multiple hydrogen bonds with *Pf*A-M17. As shown in Fig. S3B, the hydroxamate group can not only coordinate the two zinc ions, but also form four hydrogen bonds with L487, L374, D459 and L386, respectively. Moreover, three additional hydrogen bonds are observed between the amide moiety and G489, and between the ureido moiety and D459. These hydrogen bonds network together with geometric fitness in the active site could well explain the high affinity of compound **26** towards *Pf*A-M17 (K^i = 0.05 ± 0.005 μmol/L).

To preliminarily investigate the structural basis for malarial aminopeptidases selectivity of **26**, we aligned the *Pf*A-M1–**26** complex (PDB: 5XM7) on the human APN (*h*APN) structure (PDB: 4FYQ) using PyMol (http://www.pymol.org/). As shown in Fig. S4A (Supporting information), compound **26** fits well in the active site of *Pf*A-M1, with the benzyl group reaching to the S2′ region and close to the residue Y575 (also see Fig. 2). In contrast, the analogous residue of Y575 (*Pf*A-M1) is F472 in *h*APN which has a collision with the benzyl group of **26** as shown in Fig. S4B (Supporting information). The similar collision is also observed in *p*APN, which has F467 as the analogous residue (data not shown). Considering the similar volumes of phenylalanine and tyrosine, it is suggested that the different geometry of S2′ regions between *Pf*A-M1 and mammalian APNs might be the dominant factor of inhibitor selectivity. These results might in part rationalize the malarial aminopeptidases selectivity of **26**, moreover, they support our compound design strategy that inhibitors occupying S1, S1′ pockets and S2′ region simultaneously could exhibit improved malarial aminopeptidases inhibitory activity and selectivity.

To evaluate their anti-malarial activities, some compounds were selected and tested against the drug-sensitive (3D7) and drug-resistant (Dd2) strains of *Plasmodium falciparum*. The results in Table S2 (Supporting information) showed that the most potent *Pf*A-M1 and *Pf*A-M17 dual inhibitor **26** also displayed the best anti-malarial activities against both parasite strains (3D7 IC_{50} = 3.83 μmol/L, Dd2 IC_{50} = 6.38 μmol/L). The second best one among these peptidomimetic hydroxamates is compound **17**, which is also a potent *Pf*A-M1 and *Pf*A-M17 dual inhibitor. In contrast, the weak malarial aminopeptidases inhibitor **21** only exhibited marginal anti-malarial activity. Overall, the anti-malarial activities of these compounds were in line with their malarial aminopeptidases inhibitory activity. Moreover, the *Pf*A-M1 and *Pf*A-M17 dual inhibitors (**17** and **26**) possessed superior anti-malarial activities relative to the *Pf*A-M1 selective inhibitor (**15**).

Considering its significant malarial aminopeptidases selectivity and anti-malarial activity, compound **26** was progressed to *in vitro* cytotoxicity evaluation against one cancer cell line A549 (adenocarcinomic human alveolar basal epithelial cells) and one normal cell line MRC-5 (human embryonic lung fibroblasts). Satisfyingly, compound **26** inhibited A549 cells growth with IC_{50} value over 500 μmol/L, which was less cytotoxic than bestatin (IC_{50} = 487 ± 38 μmol/L) (Table S3 in Supporting information). More importantly, no significant cytotoxicity of **26** was observed against the normal cell line MRC-5 at the concentration of 500 μmol/L (Table S3), indicating the promising safety of **26**. In

contrast, the positive control doxorubicin exhibited significant cytotoxicity against both A549 (IC_{50} = 14.5 ± 2.6 μmol/L) and MCR-5 cells (IC_{50} = 22.1 ± 4.2 μmol/L) (Table S3).

To preliminarily evaluate the metabolic stability of **26**, the mouse liver microsome assay was carried out. The reduced nicotinamide adenine dinucleotide phosphate (NADPH) was used as co-factor. The results in Table S4 (Supporting information) showed that the remaining of **26** after 60 min incubation was 67%, indicating a favorable metabolic stability of **26**.

*Pf*A-M1 and *Pf*A-M17 are promising anti-malaria targets. In the present study, previously reported APN inhibitors were repositioned as *Pf*A-M1 and *Pf*A-M17 inhibitors. Cocrystal structure analysis revealed the binding modes of several representative compounds in *Pf*A-M1, which guided the rational design of more potent and selective malarial aminopeptidase inhibitors. Among the newly synthesized compounds in this study, compound **26** was demonstrated to be a potent *Pf*A-M1 and *Pf*A-M17 dual inhibitor with significant selectivity over mammalian counterpart. Structural and modeling studies rationalized the inhibitory potency and selectivity against malarial aminopepetidases of **26**. Moreover, the potent *in vitro* antimalarial potency, low host cytotoxicity and favorable mouse liver microsome stability of **26** were also confirmed. To the best of knowledge, compound **26** is the first reported *Pf*A-M1 and *Pf*A-M17 dual inhibitor with significant selectivity over mammalian APN, which provides basis for further development of selective malarial aminopepetidases inhibitors as antimalarial agents.

Declaration of competing interest

The authors declare that they have no known competing financial interests or personal relationships that could have appeared to influence the work reported in this paper.

Acknowledgments

Anil Kumar Marapaka and Priyanka Sankoju are the recipients of a fellowship from Council of Scientific and Industrial Research (CSIR), New Delhi, India. Vijaykumar Pillalamarri is supported by University Grants Commission (UGC), New Delhi, India and Bharati Reddi by Department of Science and Technology, New Delhi, India for their research fellowships. CSIR-IICT manuscript number is IICT/Pubs./2018/299. Anthony Addlagatta thanks Science and Engineering Research Board (SERB), New Delhi, India for research grants (Nos. EMR/2015/000461 and CRG/2019/006013). Yingjie Zhang thanks Natural Science Foundation of Shandong Province (No. ZR2018QH007, China), Key Research and Development Program of Shandong Province (No. 2017CXGC1401, China) and Young Scholars Program of Shandong University (No. YSPSDU, 2016WLJH33, China) for research fellowships. Renu Sudhakar is the recipient of the fellowship from the Department of Biotechnology (India). Puran Singh Sijwali lab is supported with funds from the Department of Biotechnology, India (Nos. SR/SO/BB/−0124/2012 and BT/COE/34/SP15138/2015) and the Council of Scientific & Industrial Research, India.

Supplementary materials

Supplementary material associated with this article can be found, in the online version, at doi:10.1016/j.cclet.2021.09.102.

References

[1] B. Mills, R.E. Isaac, R. Foster, J. Med. Chem. 64 (2021) 1763–1785.
[2] World Health Organization. World Malaria Report 2020; Geneva, 2020. https://www.who.int/teams/global-malaria-programme/reports/world-malaria-report-2020/.
[3] Z. Kifle, Infect. Drug Resist. 13 (2020) 4047–4060.
[4] D.E. Goldberg, A.F. Slater, A. Cerami, G.B. Henderson, Proc. Natl. Acad. Sci. U. S. A. 87 (1990) 2931–2935.
[5] J. Liu, E.S. Istvan, I.Y. Gluzman, J. Gross, D.E. Goldberg, Proc. Natl. Acad. Sci. U. S. A. 103 (2006) 8840–8845.
[6] S. McGowan, Curr. Opin. Struct. Biol. 23 (2013) 828–835.
[7] S.M. Marcin Poreba, T.S. Skinner-Adams, K.R. Trenholme, et al., PLoS One 7 (2012) e31938.
[8] S. Dalal, M. Klemba, J. Biol. Chem. 282 (2007) 35978–35987.
[9] M.B. Harbut, G. Velmourougane, S. Dalal, et al., Proc. Natl. Acad. Sci. U. S. A. 108 (2011) E526–E534.
[10] R. Deprez-Poulain, M. Flipo, C. Piveteau, et al., J. Med. Chem. 55 (2012) 10909–10917.
[11] M. Flipo, T. Beghyn, V. Leroux, et al., J. Med. Chem. 50 (2007) 1322–1334.
[12] N.B. Vinh, N. Drinkwater, T.R. Malcolm, et al., J. Med. Chem. 62 (2019) 622–640.
[13] S.N. Mistry, N. Drinkwater, C. Ruggeri, et al., J. Med. Chem. 57 (2014) 9168–9183.
[14] T.S. Skinner-Adams, C.L. Peatey, K. Anderson, et al., Antimicrob. Agents Chemother. 56 (2012) 3244–3249.
[15] N. Drinkwater, N.B. Vinh, S.N. Mistry, et al., Eur. J. Med. Chem. 110 (2016) 43–64.
[16] C. Ruggeri, N. Drinkwater, K.K. Sivaraman, et al., PLoS One 10 (2015) e0138957.
[17] K.K. Sivaraman, A. Paiardini, M. Sieńczyk, et al., J. Med. Chem. 56 (2013) 5213–5217.
[18] E. Cunningham, M. Drag, P. Kafarski, A. Bell, Antimicrob. Agents Chemother. 52 (2008) 3221–3228.
[19] T.S. Skinner-Adams, J. Lowther, F. Teuscher, et al., J. Med. Chem. 50 (2007) 6024–6031.
[20] E. Salomon, M. Schmitt, E. Mouray, et al., Bioorg. Chem. 98 (2020) 103750.
[21] L. Bounaadja, M. Schmitt, S. Albrecht, et al., Malar. J. 16 (2017) 382.
[22] G. Velmourougane, M.B. Harbut, S. Dalal, et al., J. Med. Chem. 54 (2011) 1655–1666.
[23] C. Ma, J. Cao, X. Liang, et al., Eur. J. Med. Chem. 108 (2016) 21–27.
[24] C. Ma, K. Jin, J. Cao, et al., Bioorg. Med. Chem. 21 (2013) 1621–1627.